Selected papers presented at the 14th Polish Nationwide Mössbauer Spectroscopy Seminar, OSSM'2026

Structural and Magnetic Transitions in $Bi_{0.9}La_{0.1}FeO_3$: The role of Post-Synthesis Annealing

K. Siedliska[a,*], T. Szumiata[b], R. Panek[c] and T. Pikula[a]

[a] *Lublin University of Technology, Division of Electronics and Information Technology, Nadbystrzycka 38A, 20-618 Lublin, Poland*
[b] *Casimir Pulaski Radom University, Department of Physics, Stasieckiego 54, 26-600 Radom, Poland*
[c] *Lublin University of Technology, Department of Geotechnics, Nadbystrzycka 40, 20-618 Lublin, Poland*

Doi: 10.12693/APhysPolA.150.S56 *e-mail: k.siedliska@pollub.pl

The effect of annealing temperature on the structure and magnetic properties of $Bi_{0.9}La_{0.1}FeO_3$ prepared by the sol–gel method was investigated. X-ray diffraction results showed that all samples primarily crystallize in the rhombohedral R3*c* phase, while lower annealing temperatures reduce the average crystallite size and cause a small increase in the cubic P*m*3*m* contribution. Mössbauer spectroscopy indicated that the cycloidal magnetic component is more pronounced in the spectra for samples annealed at higher temperatures, whereas the lowest-temperature sample shows stronger size-related effects. Magnetic measurements confirmed an increase in magnetization as the annealing temperature decreased. These results show that post-synthesis annealing is an important factor for controlling the structural and magnetic behavior of La-doped $BiFeO_3$.

topics: bismuth ferrite, multiferroics, spin cycloid, rare-earth doping

1. Introduction

Multiferroic materials are materials in which two or more ferroic orders, such as ferroelectricity and ferro- or antiferromagnetism, exist together and are coupled within one phase [1]. This opens interesting possibilities for applications such as multistate memories, magnetoelectric sensors, and energy-harvesting devices [2]. $BiFeO_3$ (BFO) is one of the best-known single-phase multiferroics. It shows ferroelectric behavior with $T_C \approx 1103$ K and G-type antiferromagnetic ordering with $T_N \approx 643$ K. The ferroelectric polarization is related to the lone pair electrons of Bi^{3+} ions, while Fe^{3+} ions create the antiferromagnetic sublattices, which are slightly canted due to a rhombohedral deformation of a regular perovskite structure [3]. However, in bulk BFO, the weak ferromagnetic component is modulated by an incommensurate cycloidal spin structure with a period of ≈ 62 nm. As a result, the magnetic moments are largely compensated over one cycloidal period, leading to a very small net macroscopic magnetization and a reduced linear magnetoelectric response.

A common way to improve the magnetic properties of BFO is to substitute Bi^{3+} ions with rare-earth ions, such as La^{3+}, Pr^{3+}, Nd^{3+}, or Gd^{3+}. This kind of doping changes the crystal lattice, modifies the Fe–O–Fe superexchange interactions, and can help suppress the cycloidal magnetic order. Consequently, a residual magnetic moment can appear. In addition, rare-earth doping may reduce the formation of secondary phases and lower the leakage current, which is a frequent problem in pure BFO [4]. Even so, the literature still gives some contradictions about the structural evolution of $Bi_{1-x}La_xFeO_3$ (BLFO). Many reports indicate that the rhombohedral R3*c* structure is stable up to $x \approx 0.1$, but other studies report additional or mixed phases, such as P*bam*, P*nma*, P*m*3*m*, or P4*mm* [5–8]. These differences depend strongly on the synthesis route and the thermal treatment after synthesis.

In our previous study, we showed that the cycloidal spin structure is considerably weakened at La^{3+} concentrations above 10% [7]. However, that study was limited to samples annealed at 550°C — a temperature selected based on work [9], which investigated the influence of annealing temperature

on the microstructure of pure $BiFeO_3$. Consequently, the combined effects of La substitution and annealing temperature on the structure and magnetic properties were not addressed. The aim of the present work is therefore to investigate the structural and magnetic evolution of nominal $Bi_{0.9}La_{0.1}FeO_3$ as a function of annealing temperature. To achieve this aim, X-ray diffraction (XRD), Mössbauer spectroscopy (MS), and vibrating-sample magnetometry (VSM) were used to characterize the phase composition, crystallite size, hyperfine magnetic interactions, cycloidal magnetic contribution, and macroscopic magnetic response of the samples.

2. Experimental details

Samples with the nominal composition $Bi_{0.9}La_{0.1}FeO_3$ were synthesized via the sol–gel method. Stoichiometric amounts of analytical-grade $Bi(NO_3)_3{\cdot}5H_2O$, $La(NO_3)_3{\cdot}6H_2O$, and $Fe(NO_3)_3{\cdot}9H_2O$ were dissolved in polyethylene glycol. Tartaric acid was added, and the mixture was stirred for 3 h. The obtained gel was dried at 70°C for 5 h, washed with ethyl alcohol and water to remove impurities, and then dried overnight at 120°C. The xerogels were annealed for 4 h at various temperatures (450, 500, 550, 600, and 800°C). Samples are labeled by temperature, e.g., BLFO450.

The structure of the prepared samples was verified by X-ray diffraction (XRD) using a Panalytical X'Pert Pro diffractometer in standard θ–2θ mode. For the phase and structural analyses, the *HighScore Plus* program was used.

Room-temperature Mössbauer spectra were collected in constant-acceleration mode using a POLON spectrometer in transmission geometry. A ^{57}Co source embedded in a rhodium matrix was employed to emit γ radiation with an energy of 14.4 keV. The spectrometer was calibrated using an α-Fe foil.

Magnetic measurements were conducted at ambient temperature using a vibrating sample magnetometer (VSM) capable of generating an external magnetic field of up to 14 T.

3. Results and discussion

Figure 1 shows the XRD patterns recorded for all the samples. It can be noted that all the diffractograms show characteristic peaks derived from the rhombohedral R3c $BiFeO_3$, which are marked in Fig. 1f. For the samples annealed at 600 and 800°C, small amounts of secondary phases $Bi_2Fe_4O_9$ and Bi_2O_3 were detected. However, their total contributions were estimated at ≈ 6 wt% for BLFO800 and 1.5 wt% for BLFO600. Thus, we again confirm that annealing the sol–gel-prepared BFO precursor above approximately 600°C leads to partial phase decomposition [9]. No secondary phases were detected by XRD in BLFO450, BLFO500, and BLFO550 within the detection limit of the measurement.

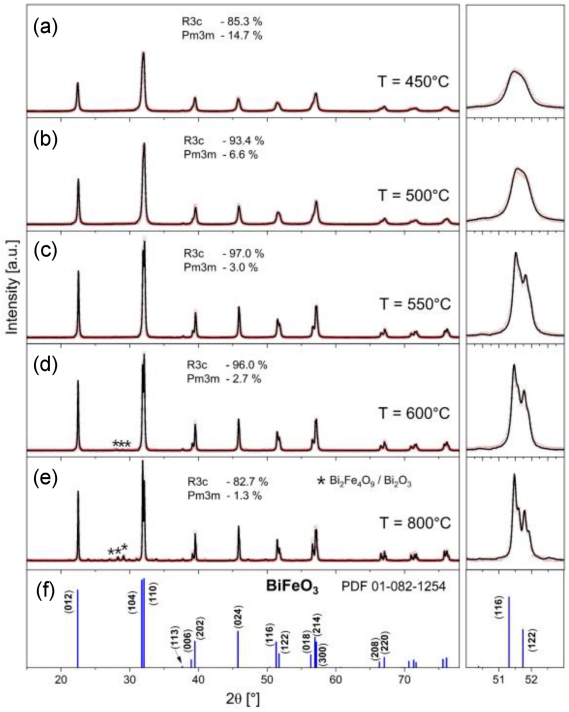

Fig. 1. (a–f) Room-temperature XRD patterns of $Bi_{0.9}La_{0.1}FeO_3$ annealed at different temperatures.

To study the crystal structure in greater detail, the Rietveld refinement method was applied. The best agreement with experimental data was achieved assuming a model consisting of a dominant rhombohedral R3c phase and a minor cubic-like P$m3m$ phase. However, the contribution of the cubic structure gradually increased from 1.3 wt% for BLFO800 to 15 wt% for BLFO450 as the annealing temperature decreased. A further consequence of lowering the annealing temperature is a decrease in crystallite size and an increase in lattice strain, as evidenced by a significant increase in the linewidths of the XRD patterns (see the right side of Fig. 1). The structural refinement revealed that BLFO550, BLFO500, and BLFO450 are nanostructured materials with average crystallite sizes of 90, 58, and 43 nm, respectively. For BLFO600 and BLFO800, the average crystallite size was much larger, exceeding 1 μm for the latter. The c lattice parameter of the R3c phase was nearly the same for all samples and equal to 1.381 nm, while the a parameter increased slightly from 0.5577 nm for BLFO800 to 0.5586 nm for BLFO450 with the drop in annealing temperature. The observed decrease in crystallite size and increase in lattice strain

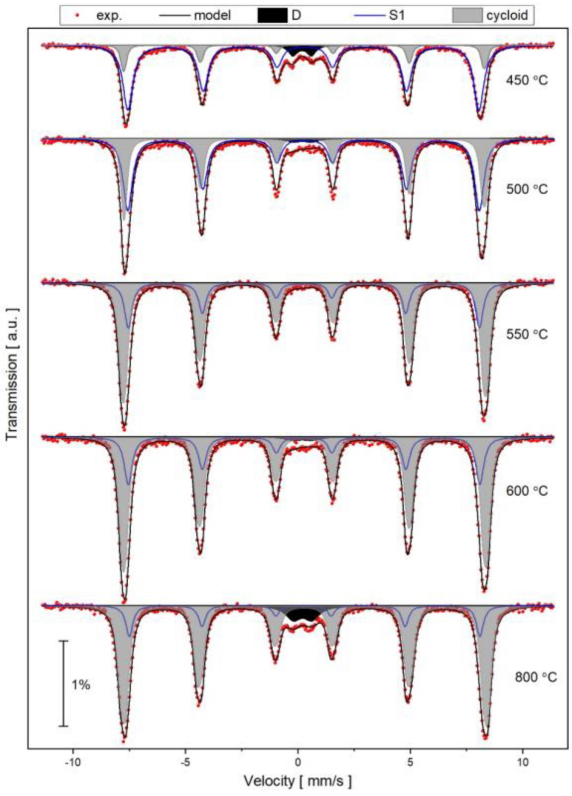

Fig. 2. Room-temperature Mössbauer spectra registered for $Bi_{0.9}La_{0.1}FeO_3$ annealed at different temperatures.

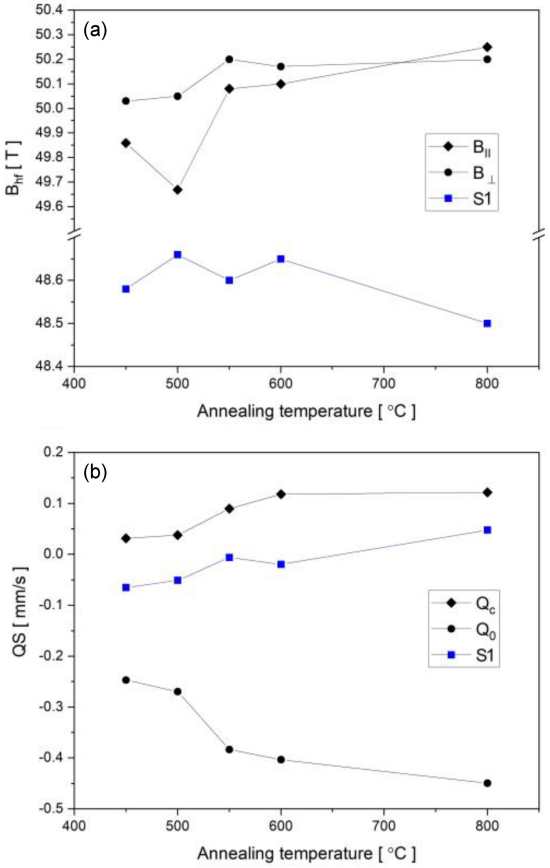

Fig. 3. Temperature dependence of the parameters derived from the fitting of Mössbauer spectra: (a) B_{hf} and (b) QS.

with decreasing annealing temperature are qualitatively consistent with the behavior reported for pure BFO samples [9].

Room-temperature Mössbauer spectra registered for BLFO annealed at various temperatures are shown in Fig. 2. Each spectrum exhibits a slightly asymmetric six-line pattern with inhomogeneous line broadening, typical of pure BFO. The spectra were fitted using the least-squares model developed by Palewicz et al. [10], which assumes variations in parameters such as:

- $B_{\|}$ and $B_{\perp}$ — hyperfine magnetic fields parallel and perpendicular to the cycloid wavevector, respectively;
- Q_0 — the amplitude of quadrupole shift (QS) modulation proportional to the electric field gradient (EFG) value and to the nuclear quadrupole moment;
- Q_c — constant component of QS corresponding to local magnetoelastic coupling;
- m — anharmonicity parameter.

To achieve optimal fitting, two additional components, the black doublet (D) and the blue sextet (S1), were included alongside the gray sextet ascribed to the cycloidal spin structure. In BLFO600 and BLFO800, the doublet likely arises from the $Bi_2Fe_4O_9$ secondary phase detected by XRD.

For BLFO450, BLFO500, and BLFO550, no secondary phases were detected by XRD, while the crystallite size drops substantially with decreasing annealing temperature. These observations indicate that the two-line component can be associated with a contribution from size-related superparamagnetic relaxation. The cycloidal component dominates in the spectrum at annealing temperatures of 500–800°C. However, for the BLFO450 sample, the S1 component with slightly reduced $B_{hf} = 48.6$ T dominates along with the doublet. The large S1 contribution in BLFO450 may reflect the combined effects of the minor $Pm3m$ contribution and the small crystallite size, which can disturb the development of the long-range cycloidal spin structure. However, above 550°C, changes become less significant, and the relative spectral area of the cycloidal component stabilizes at $\approx 70\%$. The isomer shift values for both six-line components fitted across all samples are approximately 0.39 mm/s, a typical value for Fe^{3+} ions in an oxygen environment.

Figure 3 presents the evolution of the hyperfine field and QS values as a function of annealing temperature. As annealing proceeds, the cycloidal fraction increases markedly, indicating the development

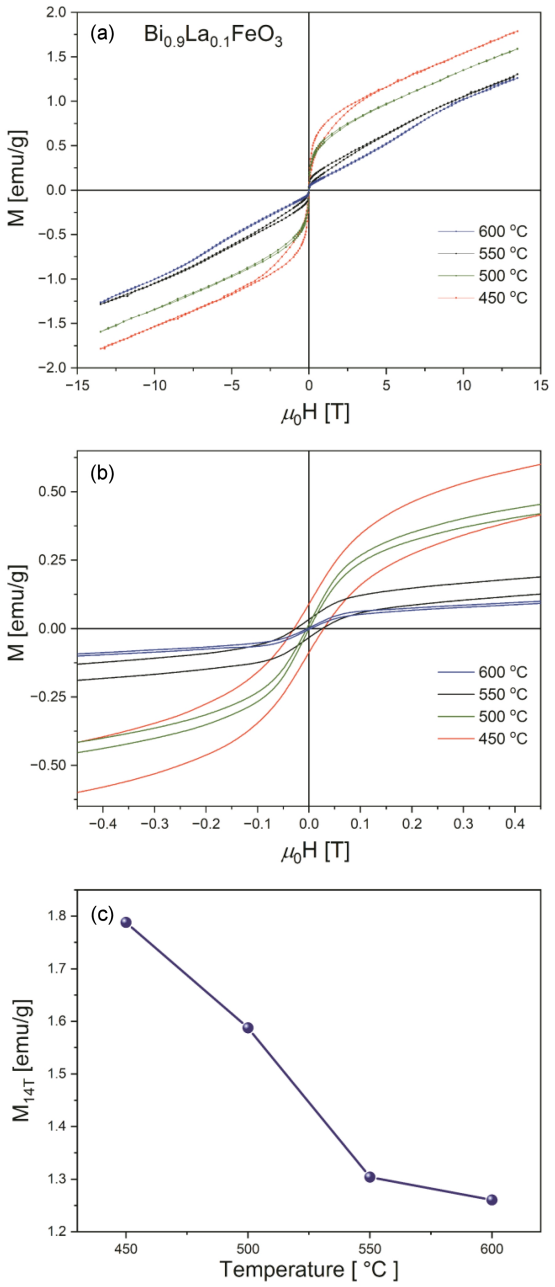

Fig. 4. (a) Room-temperature magnetic hysteresis loops of $Bi_{0.9}La_{0.1}FeO_3$ annealed at different temperatures. (b) Enlarged view of the low-field region of the hysteresis loops. (c) Magnetization at the maximum applied field of 14 T (M_{14T}) as a function of annealing temperature..

of a more coherent R3c-based magnetic structure; however, this ordering is accompanied by changes in the absolute values of Q_c and Q_0, which implies that the cycloid becomes increasingly anharmonic rather than more sinusoidal, as indicated by the rise of the anharmonicity m parameter from nearly zero for BLFO500 to 0.4959 for BLFO800. The combined trend is therefore consistent with annealing-driven relaxation of defects and strain, reduction of the superparamagnetic fraction, and a transition toward cycloidal modulation that is larger in amplitude but more anharmonic.

Figure 4 shows the magnetic hysteresis loops recorded at room temperature for all the investigated samples. It can be noted that they are superpositions of a linear (paramagnetic-like) trend and a narrow "S-type" curve characteristic of weakly ferromagnetic systems. Inset (b) in Fig. 4 shows the dependence of magnetization (M) on the annealing temperature. Since the hysteresis loops do not reach magnetic saturation within the investigated field range, the magnetization measured at the highest applied field, $H = 14$ T, was used as a reference value, M_{14T}. A substantial increase in magnetization is observed as the temperature decreases. This behavior can be explained by the systematic decrease in the average crystallite size, as determined from the XRD measurements, and is consistent with the results obtained from the Mössbauer investigations. In particular, the decrease in spectral asymmetry as annealing temperature decreases may indicate a weakening or partial suppression of the cycloidal spin structure. When the average crystallite size becomes comparable to the characteristic cycloidal period of ≈ 62 nm, the development of the long-range cycloidal modulation can be disturbed. This may lead to a stronger uncompensation of the antiferromagnetic moments and to an increase in the weak-ferromagnetic contribution. The increase in magnetization observed in the sample with the smallest crystallite sizes supports this interpretation and may also indicate a partial suppression of the cycloidal order. In addition, the wasp-waisted shape of the hysteresis loop for BLFO450 suggests the coexistence of magnetic components with different coercive fields and relaxation times. Together with the presence of the Mössbauer doublet, this behavior is consistent with a contribution from size-related superparamagnetic relaxation and provides indirect support for assigning the doublet in BLFO450 to this effect [11].

4. Conclusions

In this work, the influence of annealing temperature on the structural and magnetic properties of nominal $Bi_{0.9}La_{0.1}FeO_3$ prepared by the sol–gel method was investigated. XRD analysis confirmed that all samples primarily crystallize in the rhombohedral R3c phase, while lowering the annealing temperature leads to a smaller crystallite size, higher lattice strain, and a larger contribution from the cubic-like P$m3m$ phase. Mössbauer spectroscopy showed that the spectral contribution of the cycloidal magnetic component is more pronounced in samples annealed at higher temperatures. In contrast, the lowest-temperature sample shows a stronger contribution from the sextet associated

with fine-grain and size effects. Magnetic measurements also indicated that magnetization increases as annealing temperature decreases, which can be attributed to grain refinement and partial suppression of the cycloidal spin structure. Changes in magnetization, the Mössbauer spectral asymmetry, and the wasp-waisted hysteresis loop suggest a partial destruction of the cycloidal order and the coexistence of relaxing and more strongly blocked magnetic contributions.

References

[1] D.I. Khomskii, in: *Transition Metal Compounds*, Cambridge University Press, Cambridge, 2014, p. 269.

[2] S. Kharbanda, N. Dhanda, A.C. Aidan Sun, A. Thakur, P. Thakur, *J. Magn. Magn. Mater.* **572**, 170569 (2023).

[3] M. Fiebig, T. Lottermoser, D. Meier, M. Trassin, *Nat. Rev. Mater.* **1**, 16046 (2016).

[4] T. Durga Rao, K. Raja Kandula, A. Kumar, S. Asthana, *J. Appl. Phys.* **123**, 244104 (2018).

[5] M. Rangi, S. Sanghi, S. Jangra, K. Kaswan, S. Khasa, A. Agarwal, *Ceram. Int.* **43**, 12095 (2017).

[6] V. Antonov, I. Georgieva, N. Trendafilova, D. Kovacheva, K. Krezhov, *Solid State Sci.* **14**, 782 (2012).

[7] T. Pikula, K. Siedliska, T. Szumiata, R. Panek, V.I. Mitsiuk, L. Ruchomski, E. Jartych, *Acta Crystallogr. B Struct. Sci. Cryst. Eng. Mater.* **79**, 305 (2023).

[8] D.V. Karpinsky, I.O. Troyanchuk, M. Tovar, V. Sikolenko, V. Efimov, A.L. Kholkin, *J. Alloys Compd.* **555**, 101 (2013).

[9] T. Pikula, T. Szumiata, K. Siedliska, V.I. Mitsiuk, R. Panek, M. Kowalczyk, E. Jartych, *Metall. Mater. Trans. A Phys. Metall. Mater. Sci.* **53**, 470 (2022).

[10] A. Palewicz, T. Szumiata, R. Przeniosło, I. Sosnowska, I. Margiolaki, *Solid State Commun.* **140**, 359 (2006).

[11] L.H. Bennett, E. Della Torre, *J. Appl. Phys.* **97**, 10E502 (2005).